

## RAPID COMMUNICATIONS

*The purpose of this Rapid Communications section is to provide accelerated publication of important new results in the fields regularly covered by Journal of Materials Research. Rapid Communications cannot exceed four printed pages in length, including space allowed for title, figures, tables, references, and an abstract limited to about 100 words.*

---

### Rapid prototyping of micropatterned substrates using conventional laser printers

Michael L. Branham

*Department of Aerospace Engineering, Mechanics, and Engineering Science, University of Florida, Gainesville, Florida 32611-6250, and Department of Chemistry and Biochemistry, Florida State University, Tallahassee, Florida 32306-4390*

Roger Tran-Son-Tay

*Department of Aerospace Engineering, Mechanics, and Engineering Science, University of Florida, Gainesville, Florida 32611-6250*

Christopher Schoonover, Patrick S. Davis, and Susan D. Allen

*Department of Chemistry and Biochemistry, Florida State University, Tallahassee, Florida 32306-4390*

Wei Shyy

*Department of Aerospace Engineering, Mechanics, and Engineering Science, University of Florida, Gainesville, Florida 32611-6250*

(Received 15 November 2001; accepted 20 March 2002)

We demonstrated rapid prototyping of templates for replica molding using a conventional laser printer. A polymer, polydimethylsiloxane, was cast directly on the transparency templates to make the replicas. The templates and replicas were characterized by scanning electron microscopy, profilometry, and optical microscopy. Four patterns, including an Electronic Industries Association resolution test pattern, were printed on transparencies at 600 dots per inch on a HP LaserJet 4M printer (Hewlett-Packard, Palo Alto, CA). Optimal precision and clarity occurred between intensity settings of 50–100. Mean pattern height/depth ranged from 8–13  $\mu\text{m}$ , and width was as small as a few tenths of a millimeter. Mean surface roughness of the template patterns ranged from 1 to 4  $\mu\text{m}$  on the top surface and from 5 to 10 nm on the bare transparency surface. This method provides access to microfabricated patterns for the broader research community without the need for sophisticated micromachining facilities.

The interest in miniaturized systems for biochemical analysis and biomedical research continues to grow rapidly. Devices commonly referred to as micro total analytical systems ( $\mu\text{TAS}$ ) have been reported for a diverse range of applications, such as the determination of monoclonal antibodies,<sup>1</sup> the determination of phosphate<sup>2</sup> and nitrite,<sup>3</sup> and for high-speed DNA sequencing.<sup>4</sup> The application of similar devices to cell culture and cell mechanics<sup>5</sup> is also expanding to include the geometric control of cell shape,<sup>6</sup> orientation, and gene expression,<sup>7</sup> as well as the adhesion of neurons<sup>8</sup> and growth cone guidance.<sup>9</sup> The devices themselves usually require photolithographic microfabrication techniques to produce them since conventional machining will not provide sufficiently small devices (colloquially referred to as chips). A review by Madou provides information relating to all

aspects of microfabrication.<sup>10</sup> Chip-based devices manufactured from glass are perhaps the most widely used in part because of the versatility and chemical resistivity of glass, the relatively straightforward fabrication, and the ease of optical detection in glass devices. However, a major problem frequently encountered by researchers without specialized facilities is how to produce prototype devices rapidly and at a realistic cost.

This paper describes a practical method for the fabrication of templates, stamps, or molds using a laser printer with resolution of 600 dots per inch (dpi) or greater and solvent-free transparency film as a substrate (Fig. 1). The overall time from a computer design to a micropatterned surface is 14–24 h, most of which is for curing the polymer. No access to spin coaters, ultraviolet radiation, or tools normally found in the semiconductor process is

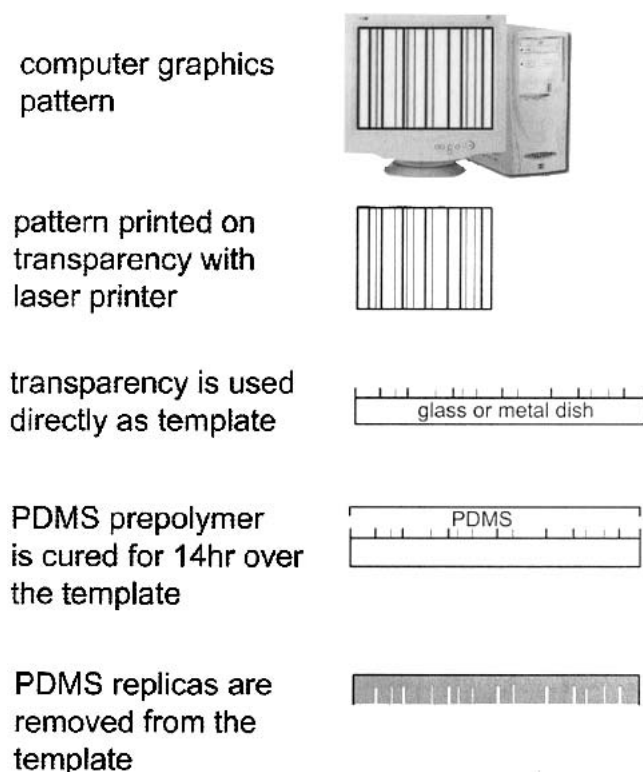


FIG. 1. Outline of the fabrication of micropatterned PDMS substrates. On the replicas, recesses are shown face down (not drawn to scale).

required, significantly reducing the cost and complexity of microengineering and micropatterned polymer surfaces. Laser<sup>11</sup> and ink-jet printers<sup>12</sup> are increasingly being used in production technologies for devices such as biosensors<sup>13</sup> and biomaterials.<sup>14</sup> The pattern resolution of the output produced by laser printers is dependent on toner particle size distribution and many other factors, e.g., the template transfer efficiency, melting, spreading, and of course the surface properties of the paper or transparencies used. For most printers, this corresponds to the maximum number of dots per inch.

Two laser printing processes are used commercially. The standard for most desktop printers (including the HP LaserJet 4M, Hewlett Packard, Palo Alto, CA) is the "write black" process, although some printers and most copiers use the "write white" process.<sup>15</sup> In the "write black" process, every spot illuminated by the laser on the print drum will be black on the print media. At each point the laser or light emitting diode array illuminates the photoconductive drum, the electrostatic charge is changed from negative to positive. As the drum continues to rotate it passes the toner cartridge that contains negatively charged finely divided toner powder, which is electrostatically attracted to the positive regions on the drum. As the paper in contact with the drum rotates, the toner is transferred to it. The paper then passes between the fusing rollers that are heated to soften low-molecular polymers in the toner and bind it to the paper.

Pattern height and aspect ratio is determined by the intensity setting on the printer, which controls the pattern charge on the drum. Pattern roughness is determined by toner particle size and fusing.

Several micropatterned polydimethylsiloxane (PDMS) substrates were produced and analyzed. Test patterns were designed with computer graphics software (Claris Draw 5.0, Claris Corp., Sunnyvale, CA) as shown in Figs. 2(a)–2(c). An EIA resolution test pattern [Fig. 2(d)] was also used to test pattern blur and continuity.<sup>16</sup> The pattern designs were then printed onto 3M (solvent free) laser color printer film using a HP LaserJet 4M printer (St. Paul, MN). PDMS was cast directly onto the transparency template after being blown dry under nitrogen gas for 5 min. The replicas were prepared from a mixture 9:1 vol% of Sylgard 184 elastomer and curing agent (Dow Chemical, Midland, MI). The mixture was then poured over the transparency templates in a glass dish and cured at room temperature for 14 h under reduced pressure to remove any air bubbles generated during mixing. The stamps were carefully removed from the master mold using a scalpel. The stamps were cleaned by vortexing in distilled water and then ethanol (95%) for 10 min each and dried under a stream of nitrogen gas.

The transparency templates and PDMS replicas were analyzed by several techniques. Bright field images were captured using an Olympus BH-2 Epifluorescent Microscope (Melville, NY) with a 10× objective and a high-resolution digital camera. Scanning electron microscope (SEM) images were obtained using a Hitachi S-4000 FE-SEM (San Jose, CA). This instrument has a maximum resolution of 1.5 nm, a magnification range of 18–300,000×, and accelerating voltage of 0.5–30 kV. Surface topography of the ink transparencies was characterized using a Tencor Alphastep 200 profilometer (Mountain View, CA) at room temperature and a scan rate of 0.02 nm/s. Atomic force microscope (AFM) scans

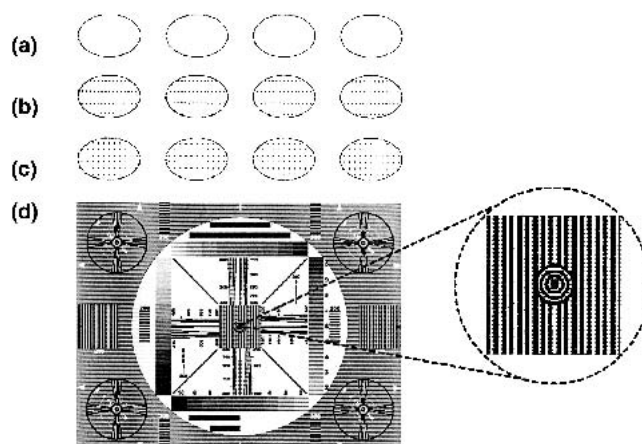


FIG. 2. Template designs: (a) ring, (b) low-density dots, (c) high-density dots, and (d) EIA resolution test pattern.<sup>16</sup>

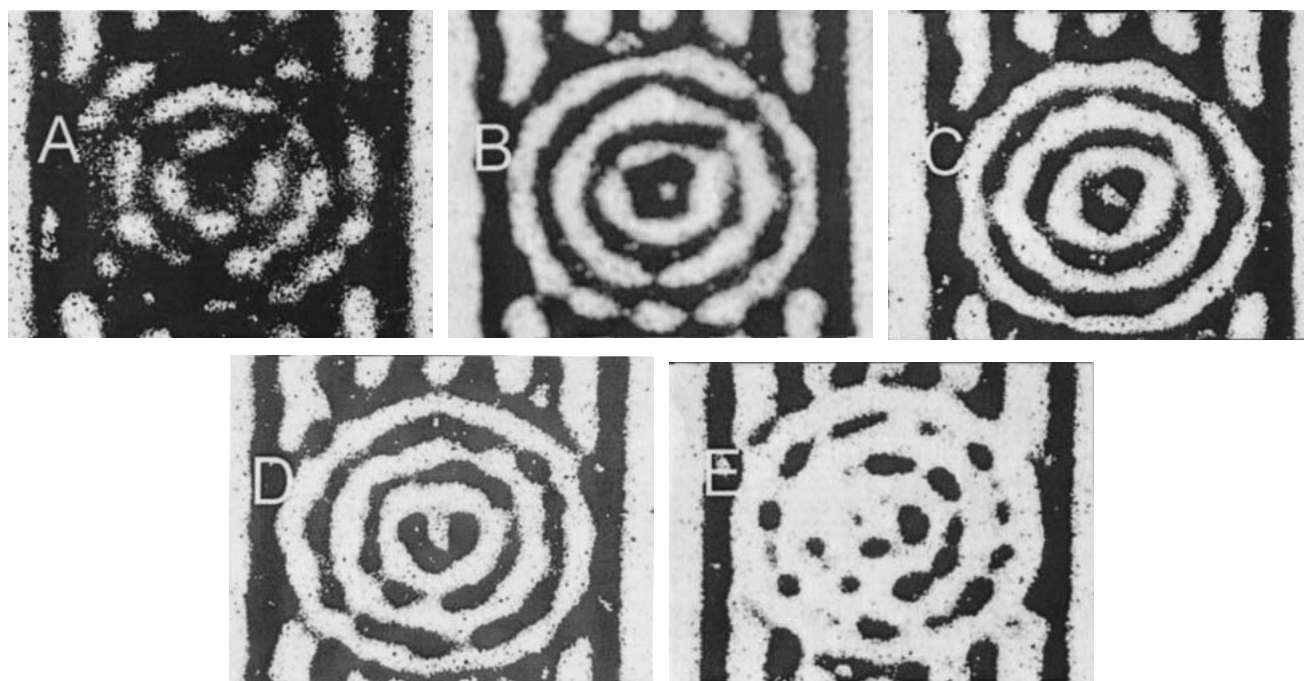


FIG. 3. Effect of decreasing print darkness on the print quality of EIA resolution pattern: (a) highest darkness (printer setting 50); (b and c) optimal precision and image clarity occurs at printer intensity settings of 50 and 100 respectively; (d) pattern begins to lose precision (printer setting 150); (e) lowest printer darkness setting (printer setting 200).

using a Digital Multimode 3000 (Digital Instruments, Santa Barbara, CA) were also performed and confirmed the profilometer surface roughness measurements. The transparency templates were stored in a laminar flow hood and blown clean with nitrogen gas prior to profilometric analysis.

The effect of print darkness settings on print quality is illustrated in Fig. 3. Micrograph 3(a) shows that at a higher print darkness setting (higher toner concentration), pattern blur occurs as larger amounts of toner are added per unit surface area. At intermediate print darkness settings 50 [Fig. 3(b)] and 100 [Fig. 3(c)] optimal precision and image clarity occurs. As observed in the image [Fig. 3(d)] at a low print darkness setting (150), the pattern begins to lose precision and break up as too little toner is used per unit surface area. At a setting of 200 [Fig. 3(e)] the clarity of the pattern is further degraded.

A SEM image of the ring pattern from Fig. 2(a) is shown in Fig. 4(a). It consists of a 600- $\mu\text{m}$ -wide toner band with irregular morphology on the surface and at the inner and outer edges of the band. The mean height of the pattern (11  $\mu\text{m}$ ) can be controlled only within a narrow range by the printer darkness settings on this printer without affecting pattern resolution. The mean surface roughness of the ring pattern is 1.2  $\mu\text{m}$ , as determined by surface profilometry [Fig. 4(b)]. The top surface Fig. 5(a) of the ring pattern contains pockets and cavities but is, as would be expected, more homogeneous than the edges

[Figs. 5(b) and 5(c)]. The edges of the ring pattern in Fig. 5(b) were found to be irregular in shape and include individual toner particles 3–8  $\mu\text{m}$  in diameter.

The minimum particle size and pattern roughness is determined from the toner particle size and/or particle fusion during the heating cycle. In Fig. 6(a), a profile of

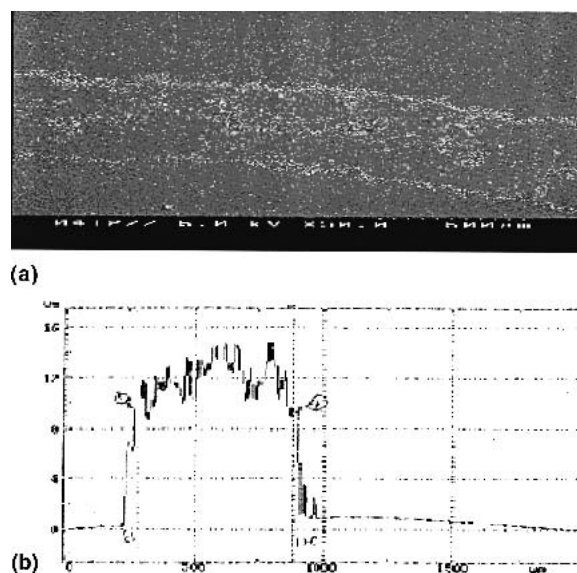


FIG. 4. Control ring dimensions. (a) Ring consists of a toner band with irregular morphology on the top surface and at the inner and outer edges of the band. (b) Ring profile shows band height (11.99  $\mu\text{m}$ ) and width (600  $\mu\text{m}$ ). Mean surface roughness of the band was 1.180  $\mu\text{m}$ .

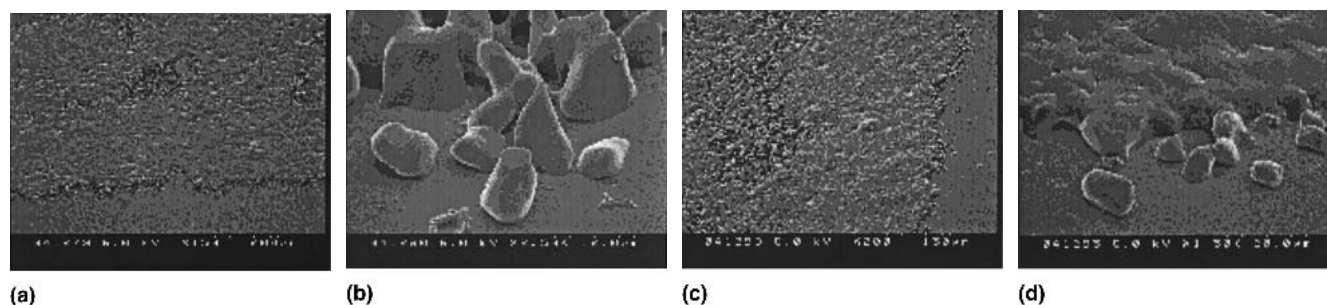


FIG. 5. SEM of ring pattern: (a) top surface; (b) edge; (c) top surface near edge; (d) pattern edge.

the “low density dots” template [pattern Fig. 2(b)] shows a surface topography that consists of a lattice structure with a average height of 7  $\mu\text{m}$ , width of 380  $\mu\text{m}$ , a pattern surface roughness of 2.5  $\mu\text{m}$ , and a transparency surface roughness of 10 nm. These templates produced in the replicas an array of microwells [Fig. 6(b)] separated by 290  $\mu\text{m}$  borders of unpatterned PDMS with nanoscale surface roughness similar to the transparency films. The “high density dot” templates [Fig. 2(c)] and replicas were very similar except that slightly deeper microwells were produced (8  $\mu\text{m}$ ) with mean bottom surface roughness of 2  $\mu\text{m}$  and top (unpatterned surface) roughness of 5 nm.

In conclusion, we demonstrated a practical method for rapid production of replica molding templates using laser printer transparencies as templates for soft lithography. This method requires no specialized microlithographic equipment or cleanroom facilities. The PDMS replicas directly cast on the laser printed templates accurately reproduce the laser printer resolution and pattern surface topography. The major disadvantages of the present method are a poor resolution and a lack of control over the depth of the patterns. However, this is a useful technique to generate microstructures with a resolution appropriate for use in bioanalytical devices or as cell

culture substrata. For example, we recently investigated the influence of substrate surface structure on epithelial cell adhesion and spreading using the described technique.<sup>17</sup> We were able to show that cellular responses to surface topography depend both on cell phenotype and microtexture of the surface in the absence of extracellular matrix proteins. In other reports, a high-resolution printer was shown capable of generating 20  $\mu\text{m}$  patterns with good quality.<sup>11,18,19</sup> Such resolution<sup>18</sup> is sufficient for many applications in biotechnology and tissue engineering where the ability to fabricate confined areas of micron scale surface roughness is desired. On the other hand, the major advantages of the method are its very low cost, versatility, ease of use, rapid turnaround time, and pattern resolution and roughness suitable for the production of substrates for cell growth and bioassays.

## REFERENCES

1. N. Chiem and D.J. Harrison, *Anal. Chem.* **69**, 373 (1997).
2. G.N. Doku and S.J. Haswell, *Anal. Chim. Acta* **382**, 1 (1999).
3. G.M. Greenway, S.J. Haswell, and P.H. Petsul, *Anal. Chim. Acta* **387**, 1 (1999).
4. S.R. Liu, Y.N. Shi, W.W. Ja, and R.A. Mathies, *Anal. Chem.* **71**, 566 (1999).
5. M.M. Peel and P. Dimilla, *Annals of Biomed. Eng.* **27**, 236 (1999).
6. C.S. Chen, M. Mrksich, S. Huang, G.M. Whitesides, and D.E. Ingber, *Science* **276**, 1425 (1997).
7. Y. Ito, *Biomaterials* **20**, 2333 (1999).
8. A.M. Turner, N. Dowell, S.W. Turner, L. Kam, M. Isaacson, J.N. Turner, H.G. Craighead, and W. Shain, *J. Biomed. Mater. Res.* **51**, 430 (2000).
9. H.C. Tai and H.M. Buettner, *Biotechnol. Prog.* **14**, 364 (1998).
10. M. Madou and J. Florkey, *Chem. Rev.* **100**, 2679 (2000).
11. T. Deng, H. Wu, S.T. Brittain, and G.M. Whitesides, *Anal. Chem.* **72**, 3176 (2000).
12. B.Y. Tay and M.J. Edirisinghe, *J. Mater. Res.* **16**, 373 (2001).
13. M. Mott, J.H. Song, and J.R.G. Evans, *J. Am. Ceram. Soc.* **82**, 1653 (1999).
14. J.D. Newman, A.P.F. Turner, and G. Marrazza, *Anal. Chim. Acta* **262**, 13 (1992).
15. R. White, in *How Computers Work*, 6th ed. (Que Publishing, Indianapolis, IN, 2002), pp. 349–386.
16. <http://www.bealecorner.com/trv900/respat/EIA1956.pdf>.
17. M.L. Branham, S.C. Glover, R.V. Benya, S.D. Allen, W. Shyy, and R. Tran-Son-Tay (2002, unpublished).
18. D. Qin, Y. Xia, and G.M. Whitesides, *Adv. Mater.* **8**, 917 (1996).
19. A. Tan, K. Rodgers, J.P. Murihy, C. O'Mathuna, and J.D. Glennon, *Lab on a Chip* 7–9, (2001).

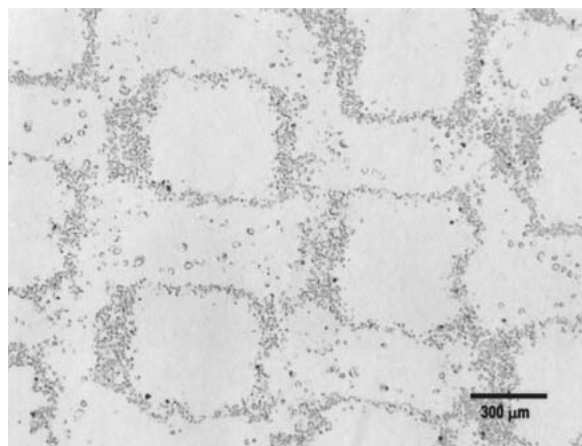


FIG. 6. Bright-field micrograph of the PDMS replica taken from the “low-density dots” pattern template in Fig. 2(b). The resulting “microwells” resemble parallelepipeds are approximately 12  $\mu\text{m}$  deep and 300–400  $\mu\text{m}$  in length.